Available online at www.sciencedirect.com
SCIENCE DIRECT®
Inorganica Chimica Acta 358 (2005) 233–238
Inorganica Chimica Acta
www.elsevier.com/locate/ica

Note

Crystal structure of the mononuclear complex [Mn(mesalim)$_2$Cl] and electrochemical studies of manganese complexes of the ligand Hmesalim

Meenal D. Godbole [a], Emanuela Grigiotti [b], Piero Zanello [b], Allison M. Mills [c], Anthony L. Spek [c], Elisabeth Bouwman [a,*]

[a] *Gorlaeus Laboratories, Leiden Institute of Chemistry, Leiden University, P.O. Box 9502, 2300 RA Leiden, The Netherlands*
[b] *Dipartimento di Chimica dell'Università di Siena, Via Aldo Moro, 53100 Siena, Italy*
[c] *Bijvoet Center for Biomolecular Research, Crystal and Structural Chemistry, Utrecht University, The Netherlands*

Received 16 July 2004; accepted 20 August 2004
Available online 23 September 2004

Abstract

The complex [Mn(mesalim)$_2$Cl] (**1**), (Hmesalim = methyl salicylimidate) has been synthesized and fully characterized. The manganese(III) complex is formed by the reaction of the ligand Hmesalim with manganese(II) chloride. Complex **1** is mononuclear and crystallizes in the space group $P\bar{1}$. Electrochemical studies were performed for complex **1**, as well as for the related complexes [Mn(mesalim)$_2$(OAc)(MeOH] · MeOH (**2**) and [Mn$_2$(etsalim)$_4$(Hetsalim)$_2$](ClO$_4$)$_2$ (**3**), (Hetsalim = ethyl salicylimidate). The complexes display intricate oxidation–reduction behaviour, and coulometric analyses in combination with electrochemical analyses have been used to understand the electron transfer mechanisms occurring at the electrodes.

Keywords: Manganese complexes; Oxidation catalysis; Electrochemistry; Crystal structures

1. Introduction

Research in the coordination chemistry of manganese is driven by the biomimetic chemistry associated with manganese present in the active sites of several enzymes [1], such as superoxide dismutase, catalase, peroxidase and photosystem II, as well as by their use as oxidation catalysts [2,3]. The principal mechanism of defence of living cells makes use of superoxide dismutase or catalase enzymes to protect the cell structure against harmful and reactive oxygen species, such as superoxide radicals or dihydrogen peroxide. There is an increasing interest in understanding the chemistry of dinuclear manganese complexes, as much structural and mechanistic information regarding the activity of the enzyme could be obtained through studies on model complexes [4,5]. Recently, we have reported good catalase activity of two manganese complexes of the ligands Hmesalim and Hetsalim (Fig. 1) [6].

In this paper, we report the synthesis and full characterization of the mononuclear complex [Mn(mesalim)$_2$Cl] (Hmesalim = methyl salicylimidate). We also report here the electrochemical studies of the series of these manganese complexes, including complex **1** and the two complexes [Mn(mesalim)$_2$(OAc) (MeOH)] · MeOH (**2**) and [Mn$_2$(etsalim)$_4$(Hetsalim)$_2$](ClO$_4$)$_2$ (**3**) (Hetsalim = ethyl salicylimidate). The ligand Hmesalim is commonly used in organic syntheses as a precursor for several other ligands [7].

* Corresponding author. Tel.: +31 71 527 4550; fax: +31 71 527 4451.
E-mail address: bouwman@chem.leidenuniv.nl (E. Bouwman).

0020-1693/$ - see front matter © 2004 Elsevier B.V. All rights reserved.
doi:10.1016/j.ica.2004.08.013

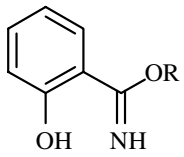

Hmesalim, R = CH_3
Hetsalim, R = CH_2-CH_3

Fig. 1. The ligands Hmesalim and Hetsalim.

2. Experimental

2.1. Materials

All reagents and solvents were used as received with no attempt to remove water or molecular oxygen. The ligand Hmesalim was synthesized using the published procedure [7–9]. The synthesis of $[Mn(mesalim)_2(OAc)(MeOH)] \cdot MeOH$ (**2**) and $[Mn_2(etsalim)_4(Hetsalim)_2](ClO_4)_2$ (**3**) has been described elsewhere [6].

2.2. Syntheses

*[Mn(mesalim)$_2$Cl] (**1**)*: 1 g (6.6 mmol) of the ligand Hmesalim was dissolved in 10 ml of methanol. 0.357 g (2.2 mmol) of solid manganese(II) chloride was added to the methanolic solution. The green solution was stirred for about 15 min; ether was added to the solution and the reaction mixture was filtered. Green crystals were obtained by slow evaporation of the solution. Yield of crude product: 80% (0.68 g), UV/VIS (CH_3CN): λ_{max} (nm) (ϵ/M^{-1} cm^{-1}) = 311 (11×10^3), 351 (6230), 421 (1120), 568 (295); IR (diamond) ν = 3263(m), 1615(s), 1590(s), 1455(m), 1393(s), 1215(s), 747(s), 521(s), 411(s) cm^{-1}; Elemental *Anal.* Calc. (%) for $C_{16}H_{16}ClN_2MnO_2$(FW = 390): C, 49.56; H, 4.16; N, 7.22; Found: C, 48.94; H, 4.08; N, 7.33%; μ_B = 4.8 BM; ESI-MS: 354.5 $\{[Mn^{III}(mesalim_2)]\}^+$.

2.3. Physical measurements

UV/Vis–NIR measurements were performed on a Perkin–Elmer Lambda 900 UV/Vis/NIR spectrometer. IR spectra were recorded on a Perkin–Elmer FT-IR Paragon 1000 spectrometer. ^1H NMR spectra were recorded on a Bruker 300 DPX MHz spectrometer. Elemental analyses were performed with a Perkin–Elmer series II CHNS/O analyzer 2400. Material and apparatus for electrochemistry have been described elsewhere [10]. All potential values are referred to the saturated calomel electrode (SCE). Under the present experimental conditions, the one-electron oxidation of ferrocene occurs at $E_{1/2}$ = +0.40 V. Electrospray mass spectra were recorded on a Thermo Finnigan AQA apparatus.

2.4. X-ray crystallographic study

Intensity data for single crystals of **1** were collected using graphite-monochromated Mo Kα radiation, on a Nonius KappaCCD diffractometer. A correction for absorption was considered unnecessary. The structure was solved by Patterson methods using DIRDIF 99 [11] and refined on F^2 using SHELXL 97 [12]. All non-hydrogen atoms were refined with anisotropic displacement parameters. All hydrogen atoms were positively identified in a difference Fourier map. All hydrogen atoms were constrained to idealized geometries and allowed to ride on their carrier atoms. All hydrogen atoms were refined with an isotropic displacement parameter related to the equivalent displacement parameter of their carrier atoms. The crystal of **1** was twinned by 180° rotation about (1 0 1); the relative fractional contributions of the two twin components are 0.738(3):0.262. Structure validation and molecular graphics preparation were performed with the PLATON package [13] (see Table 1).

3. Results and discussion

3.1. Description of the crystal structure

A PLUTON projection of the mononuclear complex **1** is shown in Fig. 2. Selected bond distances and angles are given in Table 2. Complex **1** crystallizes in the space group $P\bar{1}$. The manganese(III) ion is in a square-pyramidal geometry in an N_2O_2Cl chromophore. Two ligand molecules are bound to the metal, *trans* to each other in the square plane. The chloride ion is coordinated in the apical position at 2.422 Å. The Mn–O and Mn–N distances are typical of Mn(III). There are no hydrogen bonding, or stacking interactions present neither within

Table 1
Crystallographic data for the complex $[Mn(mesalim)_2Cl]$ (**1**)

	1
Formula	$C_{16}H_{16}ClMnN_2O_4$
fw	390.70
a (Å)	7.289(2)
b (Å)	9.675(2)
c (Å)	12.146(4)
α (°)	84.55(1)
β (°)	77.74(1)
γ (°)	71.08(1)
V (Å^3)	791.4(4)
Z	2
Space group	$P\bar{1}$
Crystal system	triclinic
ρ_{calc} (g/cm^3)	1.639
T (K)	150
μ (cm^{-1})	10.3
R (R_w)	0.052 (0.121)
S	1.18

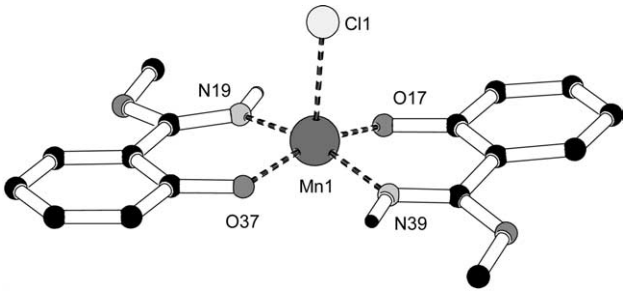

Fig. 2. PLUTON projection of [Mn(mesalim)$_2$Cl] (**1**).

Table 2
Selected bond distances (Å) and angles (°) for **1**

Atoms	Distance	Atoms	Angles
Mn(1)–N(19)	1.986(4)	N(19)–Mn(1)–O(17)	90.35(15)
Mn(1)–N(39)	1.991(4)	N(19)–Mn(1)–O(37)	86.40(15)
Mn(1)–O(17)	1.858(3)	N(39)–Mn(1)–O(17)	87.22(15)
Mn(1)–O(37)	1.846(3)	N(39)–Mn(1)–O(37)	90.40(15)
Mn(1)–Cl(1)	2.4220(17)	N(19)–Mn(1)–N(39)	163.34(17)
		O(37)–Mn(1)–O(17)	160.47(17)
		Cl(1)–Mn(1)–O(37)	98.96(12)
		Cl(1)–Mn(1)–O(17)	100.56(12)
		Cl(1)–Mn(1)–N(19)	98.44(12)
		Cl(1)–Mn(1)–N(39)	98.21(13)

the molecule nor intermolecular. The lack of interactions is unexpected and quite unusual; a bridging chloride ion would allow the formation of an octahedral geometry. Furthermore several H-bonding interactions are possible, but none are observed. The analogous complex, [Mn(mesalim)$_2$(OAc)(MeOH)] · MeOH shows the presence of a coordinated methanol molecule at the sixth coordination site on manganese and it shows extensive hydrogen bonding interactions in the crystal lattice as well [6]. The present complex **1** has the ligands bound to the metal in a *trans* manner, while the complex **2** has the two ligands bound to the metal in a *cis* geometry. The differences in ligand coordination are clearly reflected in the bond distances around manganese in the two complexes. All bonds to the ligand nitrogen and oxygens are longer in complex **2** than in complex **1** due to this difference in ligand geometries and because of the extensive hydrogen bonding interactions in complex **2** [6]. The present structure can also be compared to the [Mn(phox)$_3$] complex, which shows weaker bonds to the nitrogens and oxygens as compared to complex **1**; Mn(1)–N(21) = 2.060 and Mn(1)–O(11) = 1.882 Å in the complex [Mn(phox)$_3$] [14]. This indicates very strong bonding interactions between manganese and the ligands in complex **1**.

3.2. Spectroscopic studies

The synthesis of the complex is straightforward. In the ligand field spectra of the complex a peak at 311 nm is assigned to π–π* transitions within the ligand, because of its high intensity. The high-intensity band at 351 nm and a shoulder at 421 nm can be assigned to two LMCT transitions from the phenoxo oxygen to Mn(III) [15]. The low-intensity peak at 567 nm (ϵ = 200 mol^{-1} cm^{-1}) can be assigned to a d–d transition. In the IR spectra, the imine C=N frequency in the free ligand occurs at 1653 cm^{-1}, which shifts to 1615 cm^{-1}after complexation to Mn. The ESI-MS spectrum of the complex shows a peak at 354.5 corresponding to the molecular ion [Mn(mesalim)$_2$]$^+$. In addition peaks were also observed at 387, 505 and 744 that can be assigned to [Mn(mesalim)$_2$(MeOH)]$^+$, [Mn(mesalim)$_3$]$^+$ and [Mn$_2$(mesalim)$_4$Cl]$^+$ Room temperature magnetic measurements are consistent with the presence of Mn(III).

3.3. Electrochemistry

The electrochemistry of the complex **1** was studied along with the two analogous complexes [Mn(mesalim)$_2$(OAc)(MeOH)] · MeOH (**2**) and [Mn$_2$(etsalim)$_4$(Hetsalim)$_2$](ClO$_4$)$_2$ (**3**). These complexes, showing good catalase activity have been reported elsewhere [6].

Given the very low solubility of the present derivatives in the solvents commonly employed in electrochemical studies, only a CH$_2$Cl$_2$:MeCN (1:1) mixture appeared to give useful results.

Fig. 3 shows the cyclic voltammetric profile of the complex [Mn(mesalim)$_2$Cl] (**1**) in comparison with that of an equimolar amount of [Fe(C$_5$Me$_5$)$_2$]. Apart from the chemically reversible one-electron oxidation of decamethylferrocene (starred peaks-system; $E_{1/2}$ = −0.12 V), two irreversible oxidations appear at high potential values (E_{pa} = +1.15 V and E_{pa} = +1.39 V, respectively). The voltammetric picture remains qualitatively unaltered with scan rate, thus suggesting that in this case

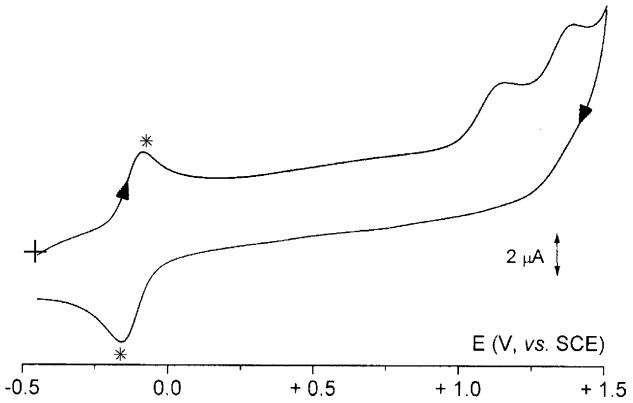

Fig. 3. Cyclic voltammogram recorded at a platinum electrode in a CH$_2$Cl$_2$:MeCN (1:1) solution containing [Mn(mesalim)$_2$Cl] (**1**), (0.7×10^{-3} mol dm^{-3}) and (0.7×10^{-3} mol dm^{-3}). [NBu$_4$][PF$_6$] (0.2 mol dm^{-3}) supporting electrolyte. Scan rate 0.2 V s^{-1}. * = [Fe(C$_5$Me$_5$)$_2$].

the second anodic process is due to the original complex. No access to the Mn(II) oxidation state was detected in the cathodic region. The closeness of the two oxidations (coupled to slight electrode poisoning effects, which required cleaning of the electrode surface after each cyclic voltammetric scan) prevented a reliable count of the number of electrons involved in these processes by controlled potential coulometry. Nevertheless, the use of $[Fe(C_5Me_5)_2]$ as an internal standard ($[Fe(C_5Me_5)_2]$ and $[Mn(mesalim)_2Cl]$ possess molecular weights not too much different, 326.3 vs. 390.4, so that their diffusion coefficients are conceivably comparable) supports that each of the two oxidations involves a one-electron transfer. The first oxidation is attributed to the irreversible Mn(III)/Mn(IV) oxidation, whereas the second oxidation is assigned to the Cl^- ligand.

Fig. 4 shows the cyclic voltammetric behaviour exhibited at a platinum electrode by the octahedral complex $[Mn(mesalim)_2(OAc)(MeOH)]$ (**2**). At relatively low scan rates, Fig. 4(a), an irreversible oxidation ($E_{pa} = +1.10$ V) precedes a second anodic process with features of partial chemical reversibility ($E_{1/2} = +1.48$ V). Controlled potential coulometry in correspondence of the (first) anodic step ($E_w = +1.25$ V) consumes one electron per molecule. Analysis of cyclic voltammograms with scan rates varying from 0.02 to 2.00 V s^{-1} shows that the process is diffusion controlled ($i_{pa} \cdot v^{-1/2}$ substantially constant) and coupled to relatively fast chemical complications (no directly associated return peak was recorded even at the highest scan rates) [16]. Also in this case, no reduction process was detected in the cathodic region down to −2 V.

As illustrated in Fig. 4(b), at high scan rates the second anodic process more or less disappears. The same happens also at very low scan rates, Fig. 4(c). These data suggest that the electrogenerated monocation instantaneously undergoes a chemical reaction to a primary product, which in turn converts to a further redox-active by-product. The overall anodic process can hence be classified as $E_iC^aC^bE_r$ mechanism. The first chemical complication C^a, which is responsible for the chemical irreversibility of the first one-electron removal (E_i), has a rate constant greater than the subsequent chemical reaction (C^b), which is responsible for the transient appearance of the second, partially chemically reversible, anodic step (E_r).

Interestingly, cyclic voltammetric tests on the exhaustively one-electron oxidised solution reveals the presence of both a new, irreversible, anodic process ($E_p = +1.50$ V) and an irreversible reduction ($E_p = -1.61$ V), which regenerates in the reverse scan the primary oxidation of the original complex, Fig. 5. On this basis, the first oxidation may be attributed to the Mn(III)/Mn(IV) passage, where after the Mn(IV) complex, being quite unstable in the original geometry, evolves to an unidentified differently coordinated species (fragmentation cannot be ruled out), which, however, upon reduction regenerates the original Mn(III) complex.

Fig. 6(a) shows the cyclic voltammetric profile of the dinuclear complex $[Mn_2(etsalim)_4(Hetsalim)_2](ClO_4)_2$ (**3**). The reaction of $Mn(ClO_4)_2$ with the mesalim ligand results in the exchange of the solvent ethoxy group with the methoxy group on the mesalim ligand during complex synthesis, thus giving the complex of etsalim ligand instead of the starting mesalim ligand [6]. As far as the anodic path is concerned, it can be seen that at low scan rates (Fig. 6(b)) a single irreversible oxidation takes place ($E_p = +1.16$ V), whereas the increase of the scan rate makes a second, essentially irreversible, anodic process to appear ($E_p = +1.51$ V), which progressively increases in intensity with scan rate. This means that the second oxidation is due to a short-lived by-product generated in the course of the main oxidation, meaning that a simple EC mechanism is operative.

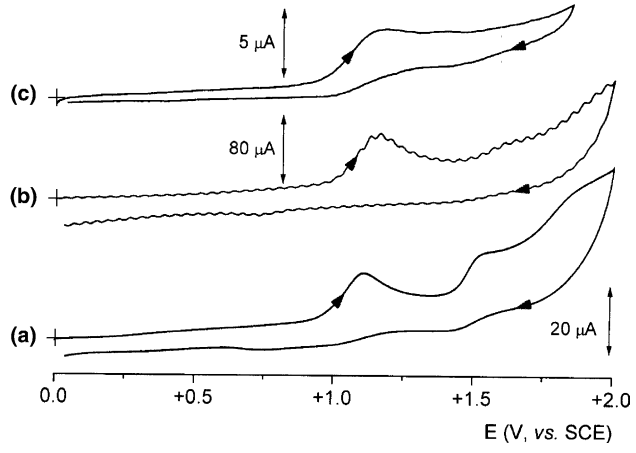

Fig. 4. Cyclic voltammogram recorded at a planium electrode in a CH_2Cl_2:MeCN (1:1) solution of $[Mn(mesalim)_2(Oac)(MeOH)]$ (**2**), (1.0×10^{-3} mol dm^{-3}). $[NBu_4]$ $[PF_6]$ (0.2 mol dm^{-3}) supporting electrolyte. Scan rate: (a) 0.2 V s^{-1}; (b) 2.0 V s^{-1}; (c) 0.02 V s^{-1}.

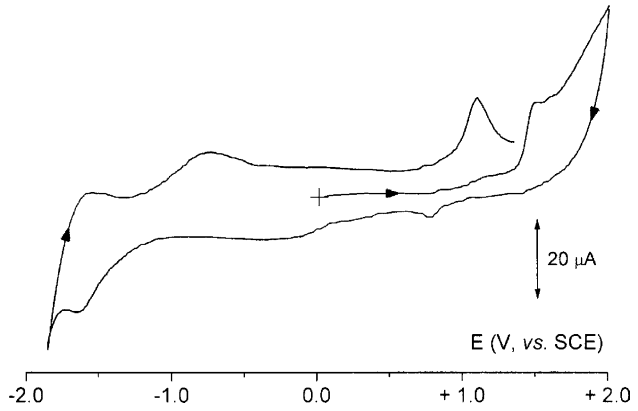

Fig. 5. Cyclic voltammogram recorded under the experimental conditions of Fig. 4, but after exhaustive one-electron oxidation (see text). Scan rate 0.2 V s^{-1}.

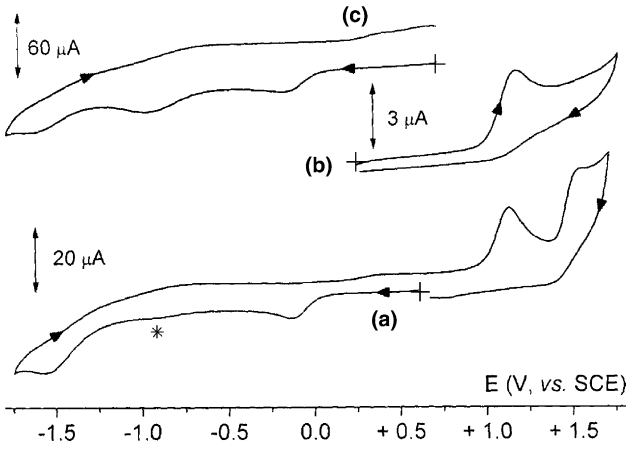

Fig. 6. Cyclic voltammograms recorded at a platinum electrode in a CH_2Cl_2:MeCN (1:1) solution of $[Mn_2(etsalim)_4(Hetsalim)_2](ClO_4)_2$ (**3**), (0.4×10^{-3} mol dm^{-3}). $[NBu_4][PF_6]$ (0.2 mol dm^{-3}) supporting electrolyte. Scan rate: (a) 0.2 V s^{-1}; (b) 0.02 V s^{-1}; (c) 2.0 V s^{-1}.

Controlled potential coulometry proved that the first step (E_w = +1.3 V) consumes two electrons *per* molecule. The pertinent cyclic voltammetric analysis showed that the current function $i_{pa} \cdot v^{-1/2}$ maintains substantially constant with scan rate and that no associated return peak was detected even at the highest scan rates. It is hence deduced that in the course of the two electron removal, the two Mn(III) centers are concomitantly oxidised to the unstable Mn(IV) oxidation state, which implies that the two manganese centres do not interact electronically upon oxidation. A different path holds as far as the reduction behaviour is concerned. In fact, at intermediate scan rates, a first irreversible process (E_p = −0.14 V) precedes a minor process (starred peak, $E_p \approx -0.9$ V), which in turn is followed by a further irreversible process (E_p = −1.56 V; the peak height roughly lies in 1:2 ratio with respect to the first reduction).

Given that the peak height of the first cathodic step is about half that of the first two-electron oxidation, it is assumed that it involves a one-electron process. Analysis of its cyclic voltammetric response with scan rate showed that the current function $i_{pc} \cdot v^{-1/2}$ maintains constant (also in this case no associated return peak was detected at the highest scan rates).

As exemplified in Fig. 6(c), in confirmation that the overall cathodic path follows a ECEC mechanism, increasing the scan rate causes a progressive increase of the minor peak at about −0.9 V (a 1:1 peak-height ratio with respect to the first step is reached at 2.0 V s^{-1}), accompanied by a progressive decrease of the most cathodic peak at −1.5 V.

Ruling out that the first two reductions might arise from deprotonation and subsequent reduction of the two protonated ligands (it is in fact conceivable that eventually a single two-electron reduction at about −0.24 V would have appeared), they are assigned to the separate Mn(III)/Mn(II) reduction of each manganese site, whereas the third reduction is attributed to the by-product originating from the chemical complications following the Mn(III) reductions.

This result suggests that upon electron addition the two manganese centres become communicating, even if the corresponding Mn(II) sites are very short lived.

In conclusion, from a simply speculative viewpoint it is proposed that the instantaneously electrogenerated (but quite elusive) mixed-valent trication $[\{(Mn^{III}–Mn^{IV}(etsalim)_4(Hetsalim)_2\}]^{3+}$ would belong to the localised Robin-Day Class I, whereas the (analogously elusive) monocation $[\{Mn^{III}–Mn^{II}(etsalim)_4(Hetsalim)_2\}]^{+}$ might belong to the delocalised Class III [17].

4. Conclusions

In this study the synthesis, and full characterization of the $[Mn(mesalim)_2Cl]$ complex is reported. We also have presented electrochemical studies of a series of three manganese complexes of the same ligand in this paper. In general, the complexes show very complex electrochemical behavior. After oxidation or reductions, the complexes transform into different structures which are unidentified at the moment. In general all complexes show partly reversible or irreversible oxidation processes at about 1.15 V assigned to Mn(III)/Mn(IV) oxidation. Reductions are generally more difficult and either irreversible or no reduction peaks were observed in these complexes. It is apparent that the ligand mesalim stabilizes the Mn(III) oxidation state. During the synthesis the oxidation of Mn(II) to Mn(III) occurs spontaneously and as yet no Mn(II) complexes could be isolated. The instability of both the Mn(II) and the Mn(IV) oxidation state complicates further studies and conclusions to be drawn for the active species in oxidation catalysis.

5. Supplementary material

Crystallographic data (excluding structure factors) for the structural analysis have been deposited with the Cambridge Crystallographic Data Centre, CCDC No. 242564. Copies of this information may be obtained free of charge from The Director, CCDC, 12 Union Road, Cambridge, CB2 1EZ, UK (fax: +44 1223 336 033; E-mail: deposit@ccdc.cam.ac.uk or www: http://www.ccdc.cam.ac.uk).

Acknowledgements

This work has been carried out within the framework of the Council for Chemical Sciences of the Netherlands Foundation for Scientific Research (CW-NWO), through a grant from the special program "Aspasia".

The authors thank Prof. Dr. Jan Reedijk for stimulating discussions. P.Z. gratefully acknowledges financial support from the University of Siena (PAR 2003).

References

[1] J. Reedijk, E. Bouwman, Bioinorganic Catalysis, Marcel Dekker Inc., New York, 1999.
[2] G.B. Shul'pin, G. Suss-Fink, L.S. Shul'pina, J. Mol. Catal. A-Chem. 170 (2001) 17.
[3] T. Katsuki, Coord. Chem. Rev. 140 (1995) 189.
[4] P.J. Pessiki, G.C. Dismukes, J. Am. Chem. Soc. 116 (1994) 898.
[5] L. Dubois, D.F. Xiang, X.S. Tan, J. Pecaut, P. Jones, S. Baudron, L. Le Pape, J.M. Latour, C. Baffert, S. Chardon-Noblat, M.N. Collomb, A. Deronzier, Inorg. Chem. 42 (2003) 750.
[6] M.D. Godbole, M. Kloskowski, R. Hage, A. Rompel, A.M. Mills, A.L. Spek, E. Bouwman, 2004, submitted.
[7] D.S.C. Black, M.J. Wade, Aust. J. Chem. 25 (1972) 1797.
[8] P. Stoss, Chem. Ber. 111 (1978) 314.
[9] P. Vinkler, K. Thimm, J. Vob, Liebigs Ann. Chem. 1976 (1976) 2083.
[10] E. Stulz, J.K.M. Sanders, M. Montalti, L. Prodi, N. Zaccheroni, F. Fabrizi de Biani, E. Grigiotti, P. Zanello, Inorg. Chem. 41 (2002) 5269.
[11] P.T. Beurskens, G. Beurskens, R. de Gelder, S. García-Granda, R.O. Gould, R. Israel, J.M.M. Smits, University of Nijmegen, The Netherlands, 1999.
[12] G.M. Sheldrick, SHELXS 97 and SHELXL 97, University of Göttingen, Göttingen, Germany, 1997.
[13] A.L. Spek, J. Appl. Crystallogr. 36 (2003) 7.
[14] M. Hoogenraad, K. Ramkisoensing, H. Kooijman, A.L. Spek, E. Bouwman, J.G. Haasnoot, J. Reedijk, Inorg. Chim. Acta 279 (1998) 217.
[15] A. Neves, S.M.D. Erthal, I. Vencato, A.S. Ceccato, Y.P. Mascarenhas, O.R. Nascimento, M. Horner, A.A. Batista, Inorg. Chem. 31 (1992) 4749.
[16] P. Zanello, Inorganic Electrochemistry. Theory, Practice and Applications, Royal Society of Chemistry, 2003.
[17] M.B. Robin, P. Day, Adv. Inorg. Chem. Radiochem. 10 (1967) 247.